Journal of Molecular Graphics and Modelling 51 (2014) 73–78

Contents lists available at ScienceDirect

Journal of Molecular Graphics and Modelling

journal homepage: www.elsevier.com/locate/JMGM

The nature of interactions in nicotinamide crystal

Tomasz Misiaszek[a,*], Żaneta Czyżnikowska[b,**]

[a] Institute of Physical and Theoretical Chemistry, Wrocław University of Technology, Wyb. Wyspiańskiego 27, 50-370 Wrocław, Poland
[b] Department of Inorganic Chemistry, Wrocław Medical University, Borowska 211, 50-556 Wrocław, Poland

ARTICLE INFO

Article history:
Accepted 17 April 2014
Available online 26 April 2014

Keywords:
Nicotinamide crystal
Intermolecular interactions
Density functional theory
Symmetry-adapted perturbation theory

ABSTRACT

In this study, we analyze the nature of intermolecular interactions in nicotinamide complexes appearing in conformations found in the crystal structure, including many-body effects. In doing so, we employ symmetry-adapted perturbation theory based on density functional theory description of monomers, and we perform the many-body variational–perturbational interaction energy decomposition. The principal finding of this study is that the stability of nicotinamide complexes is a complicated interplay of four (large in magnitude) interaction-energy components, i.e. induction, dispersion, electrostatic and exchange repulsion. However, the last two contributions cancel each other out to a large extent. In the case of considered three-body complexes, the nonadditivity effects are found to be not important. Based on the results of topological analysis of charge densities we characterized also the properties of short H ··· H contact and identified it as a weak noncovalent closed shell interaction.

1. Introduction

Nicotinamide (NAm) molecule appears to be very important precursor of many coenzymes responsible for redox processes in liver, brain and erythrocytes. Its physiological functions were recognized already in the mid-1930s, when Warburg and Christian isolated nicotinamide (NAm) from the hydrogen-transporting coenzymes NAD(H) and NADP(H), giving the first clue to its importance in metabolism [1]. About one decade later Elvehjem discovered its nutritional significance [2]. Since then NAm has been used successfully for the treatment of several deficiency conditions. One of the examples is the supplementation with NAm in the case of clinical depression. It has been shown that NAm enhances the effect of tryptophan in supporting of brain serotonin levels [3]. Nicotinamide was also found to protect high-risk children from progression of clinical insulin-dependent diabetes. It was assumed that the effect of nicotinamide involves the support of pancreatic cell function through the support of both NAD+ and DNA-protective enzyme poly(ADP-ribose) polymerase activity [4–6]. The study of Ieraci and Herrera on the ethanol-induced apoptotic neurodegeneration showed protective effect of NAm. Such properties of nicotinamide can be used to prevent the damage in fetal alcohol syndrome [7]. It is worth mentioning that nicotinamide exhibits ability to inhibit the oxidative damage. It was confirmed in the case of injury induced by reactive oxygen species whose presence can lead to oxidation of protein and lipid peroxidation. Interestingly, the protective effect was bigger than in the case of tocopherol and ascorbic acid [8]. Due to its particular importance, nicotinamide is the subject of many studies concerning its physico-chemical properties. The recent subject of interest is also the ability of nicotinamide to form co-crystals because of its well-known hydrogen-bonding moieties in the structure. The presence of two nitrogens of pyridine and amide enables to create reliable syntons with many active pharmaceutical ingredients [9–12]. Co-crystal can be defined as a crystalline structure composed of two or more different components in a stoichiometric composition stabilized by strong and directional hydrogen bonds, π–π stacking and electrostatic interactions [13]. Although co-crystals are known for a long time, it seems that their potential is not fully exploited. Due to the diversity of crystal forms, active pharmaceutical ingredients (AIP) and ability to improve their properties in clinical practice these are very attractive and challenging issues of pharmaceutical sciences. Indeed, co-crystal formation is an attractive route to modifications of physicochemical solid state properties such as stability, solubility and bioavailability without breaking or formation of covalent bonds [14–17]. It is proved that co-crystalization with nicotinamide can improve tableting behavior, dissolution performance and hygroscopic properties of drugs [18]. So far, several co-crystaline structures of nicotinamide with different AIPs have been determined. It is worth to mention here that in advance prediction if co-crystalization would be successful

* Corresponding author. Tel.: +48 713203606.
** Corresponding author. Tel.: +48 717840330.
E-mail addresses: tomasz.misiaszek@pwr.wroc.pl (T. Misiaszek), zaneta.czyznikowska@gmail.com (Żaneta Czyżnikowska).

http://dx.doi.org/10.1016/j.jmgm.2014.04.007
1093-3263/

or not is still hardly possible [19]. Therefore, it is necessary to carry out plenty of experiments under many conditions with different techniques in order to propose active form of co-crystals.

The knowledge about the non-covalent forces that cause the stabilization of a molecular crystals is one of the most important and useful elements in crystal engineering, especially in control of the stoichiometry and composition of co-crystals [20–22]. This forms the basis for the present study, which reports on the results of quantum-chemical calculations of the intermolecular interactions in nicotinamide crystals, including many-body effects. The structures were taken from Cambridge Crystal Structure Database (CSD). In doing so, we aim at providing a better understanding of the nature of binding forces in the molecular crystal to elucidate what might further contribute to the development of a strategy to predict and design the pharmaceutically relevant properties of co-crystals involving nicotinamide. Additionally, we have investigated the hydrogen bonds by means of periodic DFT calculations and atoms in molecule (AIM) theory.

2. Computational methods

2.1. DFT-SAPT calculations

In the present study, the components of the intermolecular interaction energy were obtained within the DFT-SAPT framework, which combines Kohn–Sham formulation of density functional theory (DFT) and symmetry-adapted intermolecular perturbation theory, as implemented in the MOLPRO package [23]. In this approach the total intermolecular interaction energy E_{int} is determined as a sum of first-order electrostatic energy $E_{\mathrm{el}}^{(1)}$, second-order induction $E_{\mathrm{ind}}^{(2)}$, dispersion $E_{\mathrm{disp}}^{(2)}$ and the exchange counterparts $E_{\mathrm{exch}}^{(1)}$, $E_{\mathrm{exch\text{-}ind}}^{(2)}$, $E_{\mathrm{exch\text{-}disp}}^{(2)}$, respectively:

$$E_{\mathrm{int}} = E_{\mathrm{el}}^{(1)} + E_{\mathrm{exch}}^{(1)} + E_{\mathrm{ind}}^{(2)} + E_{\mathrm{exch\text{-}ind}}^{(2)} + E_{\mathrm{disp}}^{(2)} + E_{\mathrm{exch\text{-}disp}}^{(2)} \quad (1)$$

The intramolecular charge-transfer contribution is included in $E_{\mathrm{ind}}^{(2)}$, while the exchange terms describe the repulsive effects of electron exchange between subsystems [24]. We estimated also the δ(HF) correction:

$$\delta(\mathrm{HF}) = E_{\mathrm{int}}^{\mathrm{HF}} - E_{\mathrm{el}}^{(1)}(\mathrm{HF}) - E_{\mathrm{exch}}^{(1)}(\mathrm{HF}) - E_{\mathrm{ind}}^{(2)}(\mathrm{HF}) + E_{\mathrm{exch\text{-}ind}}^{(2)}(\mathrm{HF}) \quad (2)$$

This contribution provides an estimation of higher-order induction and exchange-induction effects, that might be of particular importance for hydrogen-bonded stabilized systems. All DFT-SAPT calculations were performed assuming LPBE0AC exchange-correlation potential with a hybrid xc kernel containing 25% of exact exchange and a 75% contribution of the adiabatic local density approximation (ALDA) and with the aid of Dunning's correlation consistent aug-cc-pVDZ set (used as an atomic basis set), and the cc-pVTZ basis set which was used as the density-fitting basis [24]. In order to achieve the accuracy and to correct the wrong asymptotic behaviour of the xc potential we included the Δxc for the bulk potential which is the difference between the HOMO energy obtained from DFT calculation and the (negative) ionisation potential of the monomer (IP): The data were obtained for two sets of structures, containing two and three molecules of nicotinamide, respectively. In the latter case, trimers were described in terms of pairwise interactions.

2.2. Variational–perturbational scheme

The variational–perturbational scheme was applied in order to estimate the importance of nonadditivity of interactions in the case of nicotinamide complexes in orientations appearing in the crystal structure. In this approach the total intermolecular energy and all of its components are basis set superposition error free due to the counterpoise correction. At the MP2 level of theory, the total intermolecular interaction energy of a 3-body complex can be decomposed in the following way [25,26]:

$$\Delta E^{\mathrm{MP2}} = \Delta E^{\mathrm{HF}} + \epsilon_{\mathrm{el,r}}^{(12)} + \epsilon_{\mathrm{disp}}^{(20)} + \Delta E_{\mathrm{exch\text{-}del,2}}^{(2)} + \Delta E_{\mathrm{exch\text{-}del,3}}^{(2)} \quad (3)$$

where $\epsilon_{\mathrm{disp}}^{(20)}$ is the second order dispersion interaction; $\epsilon_{\mathrm{el,r}}^{(12)}$ describes the electron correlation correction to the first order electrostatic interaction and the remaining electron correlation effects are encompassed in the $\Delta E_{\mathrm{ex}}^{(2)}$ term. ΔE^{HF} is the intermolecular interaction energy at the HF level of theory:

$$\Delta E^{\mathrm{HF}} = \epsilon_{\mathrm{el}}^{(10)} + \epsilon_{\mathrm{exch,2}}^{\mathrm{HL}} + \epsilon_{\mathrm{exch,3}}^{\mathrm{HL}} + \Delta E_{\mathrm{del,2}}^{\mathrm{HF}} + \Delta E_{\mathrm{del,3}}^{\mathrm{HF}} \quad (4)$$

$\epsilon_{\mathrm{el}}^{(10)}$ is the electrostatic interactions of unperturbed monomer charge densities; $\Delta E_{\mathrm{ex}}^{\mathrm{HL}}$ stands for the associated exchange repulsion and ΔE_{del} is the delocalization component. Moreover variational–perturbational scheme was applied in order to estimate the 2-body interactions in the considered crystal. All calculations of the decomposition of intermolecular interaction energy at the MP2/aug-cc-pVDZ level of theory were performed using the modified version of the GAMESS US package [27–31].

2.3. Atoms in molecules method

In the present study, the topological properties of electron density in the considered complexes were assigned using the Quantum Theory of Atoms in Molecules (QTAIM) of Bader [32,33].

We estimated the properties of bond critical points (BCPs) localized at the bond path linking the interacting species, especially the electronic density at BCP, $\rho(\mathbf{r}_{\mathrm{BCP}})$, and its Laplacian, $\nabla^2\rho(\mathbf{r}_{\mathrm{BCP}})$. It is known that negative values of $\nabla^2\rho(\mathbf{r}_{\mathrm{BCP}})$ imply concentration of electronic charge in the intermolecular region and its magnitude yields the information about the strength of interactions of considered systems. The positive values of Laplacian, in turn, correspond to the reduction of electronic charge in the intermolecular region.

The local kinetic $G(\mathbf{r}_{\mathrm{BCP}})$, potential $V(\mathbf{r}_{\mathrm{BCP}})$ and total $H(\mathbf{r}_{\mathrm{BCP}})$ energy densities, estimated at the bond critical point can be also useful in analysis of the weak intermolecular interactions. The electronic energy density of the local charge distribution may be calculated as the sum of the local kinetic and potential energy densities:

$$H(\mathbf{r}_{\mathrm{BCP}}) = G(\mathbf{r}_{\mathrm{BCP}}) + V(\mathbf{r}_{\mathrm{BCP}}) \quad (5)$$

The AIM calculations were performed using the AIM2000 program [34].

2.4. Solid state DFT calculation

Optimization, atom positions and the unit cell parameters of NAm were performed using the CRYSTAL09 software package [35] using density functional theory and based on the linear combination of atomic orbitals (LCAO) method. In this work we tested four functionals, namely local density approximation (LDA), PBE, developed for solids PBEsol and B3LYP hybrid functional with the 6-311G(d,p) basis set obtained from the EMSL basis-set library [36,37]. Grimme's approach was used to include long-range dispersion contributions to the DFT total energy and gradients at the B3LYP level of theory. Van der Waals radii and atomic coefficients were taken from [38] and [39] for B3LYP-D and B3LYP-D* respectively. We applied isotropic shrinking factors of 4 and 4 for the Monkhorst–Pack and Gilat k-point net, respectively. Values of 8, 8, 8, 8 and 16 were employed as truncation criteria for the bielectronic integrals. An energy convergence criterion of 10^{-9} a.u. was used in

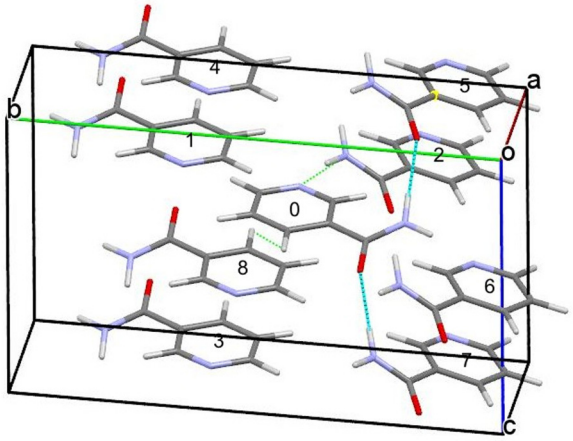

Fig. 1. The structure of complexes considered in energy partitioning calculations.

the self-consistent field iteration for optimization. The initial crystal structure was taken from [40].

3. Results and discussion

NAm crystallizes in the monoclinic space group P21/*c* with four molecules in the unit cell (see Fig. 2). The molecules are linked by NH · · · O HB along *c* axis. On the other hand, the amino group forms a hydrogen bond with the nitrogen atom of the pyridine ring. It has been also revealed that there is a short H · · · H contact of 1.979 length which is below the sum of the van der Waals radii.

It was reported for the first time by Wright et al. in 1954 that the structure of nicotinamide crystal is stabilized by two weak hydrogen bonds [41]. The first one, of length 2.99 Å, involves nitrogen atom of amino group and oxygen atom, while the second one, of length 3.09 Å, is localized between two nitrogens of amino group of subsequent molecules [41]. Similar results, albeit much more accurate, were obtained by Miwa et al. [40]. Apart from the structure, these authors determined the electron distribution and electrostatic potential in the nicotinamide crystal. They determined crystal structure from X-ray (at 150 K and 295 K) and neutron diffraction experiments (at 295 K). The accurate positions of H atoms were found by referring to the results of the neutron diffraction study and further we will relate to this structure. The exact positions of H atoms allow us to validate the accuracy of the DFT functional for the prediction of lattice and HB parameters. In Table 1 there are collected structure parameters (lattice constants and angle) calculated with different functionals compared with experimental results. The most remarkable deviations are observed for LDA, PBE and B3LYP. The most popular functional B3LYP overestimates the length of a parameter about 40%. B3LYP with dispersion corrections (B3LYP-D and B3LYP-D*) give smaller discrepancies. The next functional, PBEsol designed for solids, provides by far the best lattice parameters with percentage errors smaller than 1% in the case of *a*, *b* and angle β, whereas the length of *c* axis is overestimated about 3%. This shows that dispersion correction is crucial for this system and generally for molecular crystals. Table 2 refers to the HB geometries and H · · · H distance. The calculated results show better agreement with those experimental ones with deviation below 5%. As it can be expected worse agreement was found for LDA and PBE.

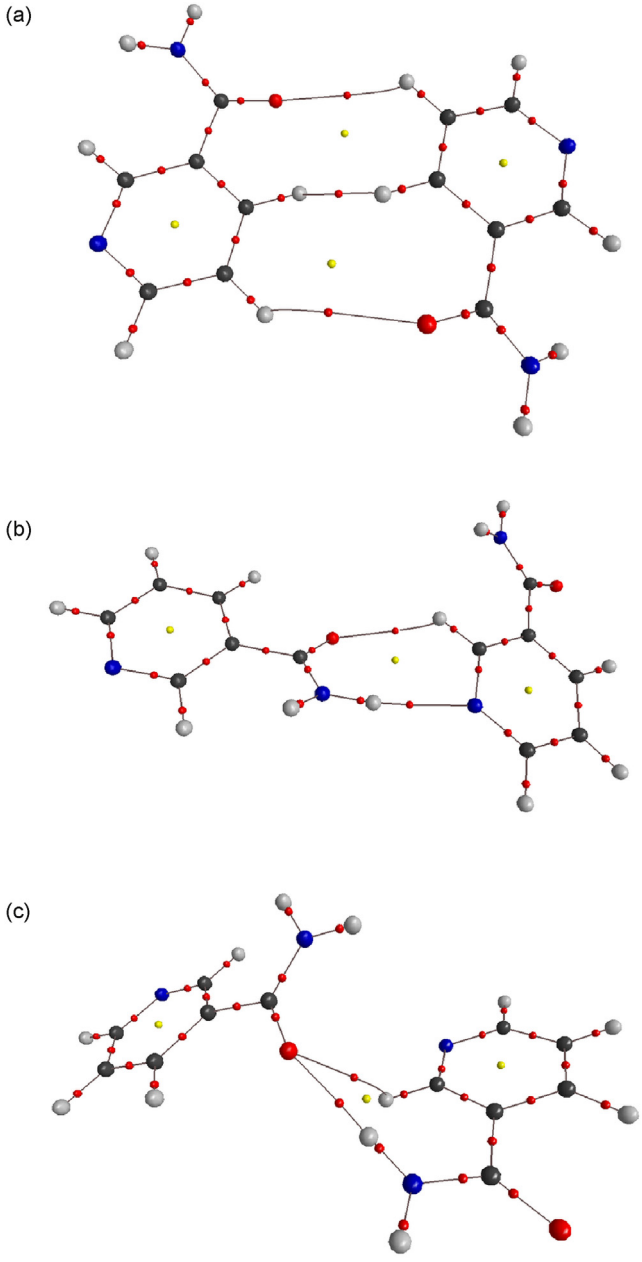

Fig. 2. BCP (red) for (a) H · · · H interaction (structure 0 . . . 3), (b) NH · · · N (structure 0 . . . 2) and (c) NH · · · O (structure 0 . . . 5) hydrogen bonds. (For interpretation of the references to color in this figure legend, the reader is referred to the web version of the article.)

Table 1
The comparision of structural parameter of NAm crystal.

	a/Å	*b*/Å	*c*/Å	β/°	*V*/Å^3
LDA	3.683	14.989	8.976	96.37	492.49
PBE	5.345	14.539	8.890	98.13	683.95
PBEsol	3.968	15.670	9.145	98.23	562.73
B3LYP	5.531	14.651	9.045	100.06	721.81
B3LYP-D	3.642	15.014	9.285	95.70	505.27
B3LYP-D*	3.782	15.377	9.271	95.99	536.23
Exp.	3.975	15.632	9.422	99.03	578.20

Table 2
Geometry parameters of the intermolecular hydrogen bonds and H···H distance (distances are given in Å, angles in °).

	*r*NH···O	<NH···O	*r*NH···N	<NH···N	*r*H···H
LDA	2.788	175.38	2.862	168.34	2.756
PBE	2.918	168.24	2.988	176.49	2.599
PBEsol	2.853	176.11	2.939	169.24	1.981
B3LYP	2.951	168.01	3.050	176.63	2.756
B3LYP-D	2.946	175.54	2.997	167.74	1.867
B3LYP-D*	2.943	175.64	3.033	168.34	1.864
Exp.	2.994	175.15	3.104	168.83	1.979

PBEsol functional predicts the H···H distance with an error 0.10%, whereas it underestimates HB lengths by about 5%. Because B3LYP predicts dramatically enlarged unit cell size it can be expected that the intermolecular distances will be increased. Indeed, the H ··· H distance amount to 2.756 Å, but the HB geometries are well reproduced. B3LYP functionals with dispersion correction (D2 and D*) give result with errors not exceeding 3.5% in the case hydrogen bonding parameters and slightly above 5.5% in the case H ··· H distance.

It is also worth to mention that, according to the crystallographic data, the molecular stacks are separated by 3.58 Å. Consequently, based on the available literature concerning the nature of intermolecular interactions in organic compounds in stacked alignments and involved in hydrogen bonding, the complicated interplay of various types of interaction energy components should be expected [42–44]. First of all, the sources of stability can be seen in interaction of the permanent and induced electric multipole moments due to their mutual polarization [42–44]. Matta et al. suggested that in organic crystals such short contacts may result in closed shell interactions between adjacent hydrogen atoms [45]. Hence, it is particularly interesting to determine the impact of aforementioned contact on the crystal structure of nicotinamide [see pair 0 . . . 8 in Fig. 1]. In order to verify this assumption, in the present study we considered pairs of structures in line and slope configurations to characterize hydrogen bonded and H ··· H interactions, respectively. Since geometric criteria are not sufficient for the justification of HB we performed AIM analysis based on topological analysis of charge density, $\rho(r_{BCP})$, its Laplacian, $\nabla^2\rho(\mathbf{r}_{BCP})$, local electronic energy density, $G(\mathbf{r}_{BCP})$, local potential energy density $V(\mathbf{r}_{BCP})$ and hence total local energy density, $H(\mathbf{r}_{BCP})$ at bond critical point (BCP). Table 3 presents the topological parameters at BCPs for the intermolecular HBs studied here. It can be seen that $\rho(r_{BCP})$ and $\nabla^2\rho(\mathbf{r}_{BCP})$ values for HBs fall into the range of typical values for moderate HBs. According to the set of topological criteria proposed by Bader and Essen [46] and Koch and Popelier [47] we found that HBs belongs to weak noncovalent closed shell interactions.

Table 4 contains the results of intermolecular interaction energy partitioning performed using DFT-SAPT (cf. Eq. (1)). The presented data were obtained for conformations of dimers and dimer-like trimers corresponding to these found in crystal [40]. The data concern the interactions between molecules **0** and **1**, **0** and **2**, respectively. The numbers of monomers correspond to those shown in Fig. 1. Furthermore, the dimer denoted as **02** . . . **5** is the case where the molecules **0** and **2** are treated as a monomer and molecule **5** as the second one. According to the received results the magnitude of the total intermolecular energy varies significantly in the case of analysed set of structures. In the case of both SAPT-DFT and MP2 outcomes the stability of pair **0** . . . **1** and **0** . . . **4** is rather small and varies from −1.9 to −3.11 kcal/mol. Whereby, the values of the total intermolecular interaction energy obtained using the variational–perturbational scheme receiving slightly lower value. So weak interactions results from the mutual arrangement of the monomers in the considered pairs. In the case of **0** . . . **1** the molecules lie in the line alignment and the distance between closest atoms ($N_0 \cdots H_1$—C_1) is about 2.7 Å. The **0** . . . **4** pair is stabilized by H—H contact and the distance between hydrogens is lower than 2 Å. For both molecular layouts of complexes discussed above, the stabilization origins from second-order components, namely dispersion and induction. Even though first-order electrostatic energy has a negative value, it is completely cancelled out by associated exchange-repulsion component. Among the analysed set of structures, the value of the total intermolecular interaction energy calculated for **02** . . . **5** is the most negative one. This is complex where nicotinamide molecules are in almost stacked alignments. This kind of spatial arrangement might imply large values of dispersion energy. As far as the structure **02** . . . **5** is concerned, the distance between the perpendicular planes of nicotinamide rings is about 3.5 Å. In this case, the induction and dispersion energies estimated using SAPT-DFT method are the most substantial stabilizing factors and both are similar value. It should be mentioned that charge-transfer energy is covered in the former term. The results

Table 3
Topological parameters for intramolecular interaction in (3): electron density ($\rho(r_{BCP})$), Laplacian of electron density ($\nabla^2\rho(\mathbf{r}_{BCP})$), electron kinetic energy density ($G(\mathbf{r}_{BCP})$), electron potential energy density ($V(\mathbf{r}_{BCP})$), total electron energy density ($H(\mathbf{r}_{BCP})$), hydrogen bond energy (EHB) at bond critical point (BCP).

	$\rho(r_{BCP})$	$\nabla^2\rho(\mathbf{r}_{BCP})$	$G(\mathbf{r}_{BCP})$	$V(\mathbf{r}_{BCP})$	$H(\mathbf{r}_{BCP})$
H ··· H (0 . . . 3)					
C—H ···H—C	0.0111	0.0356	0.0072	−0.0056	0.0017
C—H ···O	0.0028	0.0102	0.0021	−0.0015	0.0005
NH ··· N (0 . . . 2)					
N—H ···N	0.0212	0.0652	0.0144	−0.0126	0.0019
C—H ···O	0.0089	0.0271	0.0060	−0.0052	0.0008
NH ··· O (0 . . . 5)					
N—H ···O	0.0194	0.0832	0.0174	−0.0140	0.0034
C—H ···O	0.0087	0.0288	0.0063	−0.0054	0.0009

Table 4
The results of intermolecular interaction energy partitioning. The data were obtained using SAPT-DFT and are given in kcal/mol.

Complex	$E^{(1)}_{pol}$	$E^{(1)}_{exch}$	$E^{(2)}_{ind}$	$E^{(2)}_{ind\text{-}exch}$	$E^{(2)}_{disp}$	$E^{(2)}_{disp\text{-}exch}$	$E^{(1)}$	ΔHF	$E^{(2)}$	E_{int}
0 . . . 1	−2.74	2.96	−0.85	0.47	−3.06	0.33	0.21	−0.24	−3.10	−2.89
0 . . . 2	−10.37	10.14	−4.97	2.90	−5.53	0.89	−0.23	−1.30	−6.71	−6.94
0 . . . 3	−3.69	4.39	−1.39	0.88	−5.08	0.53	0.70	−0.42	−5.05	−4.35
0 . . . 4	−1.51	2.97	−0.92	0.74	−3.61	0.40	1.46	−0.27	−3.37	−1.90
0 . . . 5	−9.33	8.74	−3.95	2.03	−5.59	0.77	−0.59	−1.08	−6.73	−7.32
02 . . . 5	−19.10	18.79	−9.15	4.93	−11.00	1.69	−0.30	−2.57	−13.53	−13.83
03 . . . 8	−5.85	8.13	−2.62	1.46	−8.82	0.91	2.28	−0.73	−9.07	-6.79

Table 5
The results of intermolecular interaction energy partitioning. The data were obtained at the MP2/aug-cc-pVDZ level of theory and are given in kcal/mol.

Number	$\epsilon^{(10)}_{el}$	$\epsilon^{HL}_{ex,2}$	$\Delta E^{HF}_{del,2}$	$\epsilon^{(12)}_{el,r}$	$\epsilon^{(20)}_{disp}$	$\Delta E^{(2)}_{ex\text{-}del,2}$	ΔE^{HF}	ΔE^{MP2}
0 . . . 1	−2.82	2.56	−0.63	0.00	−3.03	0.80	−0.88	−3.11
0 . . . 2	−10.50	9.09	−3.46	−0.18	−5.32	2.29	−4.88	−8.08
0 . . . 3	−4.23	4.47	−1.01	0.37	−5.59	1.09	−0.77	−4.90
0 . . . 4	−1.74	3.24	−0.47	−0.02	−4.25	0.78	1.01	−2.47
0 . . . 5	−10.15	7.79	−3.18	1.09	−5.72	1.99	−5.54	−8.18
02 . . . 5	−20.02	16.65	−7.13	0.87	−11.03	4.40	−10.50	−16.25
03 . . . 8	−6.35	7.78	−2.12	−0.68	−9.56	2.14	−0.68	−7.92

Table 6
The many-body intermolecular interaction partitioning energy of nicotiamide triplex estimated using variational–perturbational scheme at the HF and MP2 level of theory. The data are given in kcal/mol.

	1 mb (0...1...4)	2 mb (0...2...5)	3 mb (0...3...7)
$\epsilon_{el}^{(10)}$	−4.22	−20.28	−6.25
$\epsilon_{HL}^{ex,2}$	11.03	22.09	13.20
$\epsilon_{ex,3}^{HL}$	−0.06	−0.09	−0.13
$\Delta E_{del,2}^{HF}$	−1.78	−7.32	−2.58
$\Delta E_{del,3}^{HF}$	−0.013	0.005	−0.015
$\epsilon_{el,r}^{(12)}$	−0.82	0.11	−0.51
$\epsilon_{disp}^{(20)}$	−17.36	−21.15	−19.67
$\Delta E_{ex\text{-}del,2}^{(2)}$	2.97	5.69	3.40
$\Delta E_{ex\text{-}del,3}^{(2)}$	0.06	0.14	0.091
ΔE^{HF}	4.96	−5.59	4.23
ΔE^{MP2}	−10.19	−20.81	−12.46

obtained at the MP2 level of theory indicated also that the most stabilizing components are dispersion and delocalization (see Table 5). The magnitude of first-order energy has small destabilizing character due to the mutual cancellation of electrostatic and exchange terms. It confirms that such pattern of intermolecular interaction components is characteristic for molecules with heterocyclic ring in their structure in stacked alignments. The higher-order induction contribution are the largest for **02** ... **5** molecular layout (cf. the most negative value of δ(HF)).

The data collected in Table 6 reveal that the many-body effects are not substantial, since their contribution to the total intermolecular interaction energy does not exceed 1%. In the case of all studied systems, the three-body contributions to the HF interaction energy are quite small in comparison with the two-body terms. It can be also observed that the exchange repulsion is found to be practically pairwise additive for all analyzed complexes.

4. Summary

Intermolecular interactions in the crystal structure of nicotinamide were studied within the DFT framework and using the MP2 method. Periodic DFT calculations of the NAm structure has revealed that that including the long-range dispersion corrections gives reasonable agreement with lattice parameters as well as hydrogen bonding geometry. According to the DFT-SAPT results, the dispersion, induction and electrostatic interactions are found to be the most important stabilizing factors. The latter component of interaction energy is cancelled to a large extent by the associated Pauli exchange repulsion. It is confirmed by the data obtained using variational–perturbational scheme which indicate that the dispersion and delocalization energies stabilizing nicotinamide crystal structure. The analysis of three-body complexes demonstrated that many-body effects in interactions in nicotinamide crystal are negligible. Moreover, it was confirmed that stabilization of many-body complexes originates mainly from the second-order components. Finally, it should be also emphasized that theoretical studies, concerning the decomposition of nonadditivity of intermolecular interactions, are scarcely available. Hence, the results presented herein are a step towards filling this gap.

Acknowledgments

This work was supported by computational grant from Wroclaw Centre for Networking and Supercomputing (WCSS). The allocation of computing time is greatly appreciated. The authors are grateful to Dr. P. Lipkowski for his help in QTAIM calculations. Z.C. thanks for the statutory activity subsidy from Polish Ministry of Science and Higher Education for the Wroclaw Medical University (ST-704). T.M. acknowledges financial support from the statutory activity subsidy from the Polish Ministry of Science and Higher Education for the Faculty of Chemistry of Wroclaw University of Technology (S300158/I-30).

References

[1] O. Warburg, Biochemistry 287 (1936) 291.
[2] C. Elvehjem, R. Madden, F. Strong, D. Woolley, The isolation and identification of the anti-black tongue factor, Nutr. Rev. 32 (2) (1974) 48–50.
[3] Y. Tian, D. Li, Q. Ma, X. Gu, M. Guo, Y. Lun, W. Sun, X. Wang, Y. Cao, S. Zhou, Excess nicotinamide increases plasma serotonin and histamine levels, Acta Physiol. Sin. 65 (2013) 33–38.
[4] S. Reddy, N. Bibby, R. Elliott, Early nicotinamide treatment in the nod mouse: effects on diabetes and insulitis suppression and autoantibody levels, Diabetes Res. 15 (2) (1990) 95–102.
[5] Y. Yonemura, T. Takashima, K. Miwa, I. Miyazaki, H. Yamamoto, H. Okamoto, Amelioration of diabetes mellitus in partially depancreatized rats by poly(adp-ribose) synthetase inhibitors. Evidence of islet b-cell regeneration, Diabetes 33 (4) (1984) 401–404.
[6] H. Elliott, R.B. Chase, Prevention or delay of type i diabetes mellitus in children using nicotinamide, Diabetologia 34 (1991) 362–365.
[7] A. Ieraci, D. Herrera, Nicotinamide protects against ethanol-induced apoptotic neurodegeneration in the developing mouse brain, PLoS Med. 3 (4) (2006) 547–557.
[8] J. Kamat, T. Devasagayam, Nicotinamide (vitamin b-3) as an effective antioxidant against oxidative damage in rat brain mitochondria, Redox Rep. 4 (4) (1999) 179–184.
[9] L. Benyong, H. Shuling, Different hydrogen-bonded interactions in the cocrystals of nicotinamide with two aromatic acids, J. Chem. Crystallogr. 41 (11) (2011) 1663–1668.
[10] S. Nicoli, S. Bilzi, P. Santi, M. Caira, J. Li, R. Bettini, Ethyl-paraben and nicotinamide mixtures: apparent solubility, thermal behavior and X-ray structure of the 1:1 co-crystal, J. Pharm. Sci. 97 (11) (2008) 4830–4839.
[11] N. Cheney, M.L. Shan, E. Healey, M. Hanna, L. Wojtas, M. Zaworotko, V. Sava, S. Song, J. Sanchez-Ramos, Effects of crystal form on solubility and pharmacokinetics: a crystal engineering case study of lamotrigine, Cryst. Growth Des. 10 (2010) 394–405.
[12] J.I. Arenas-Garcia, D. Herrera-Ruiz, K. Mondragon-Vasquez, H. Morales-Rojas, H. Hopfl, Co-crystals of active pharmaceutical ingredients-acetazolamide, Cryst. Growth Des. 10 (2010) 394–405.
[13] A. Jayasankar, A. Somwangthanaroj, Z. Shao, N. Rodrguez-Hornedo, Cocrystal formation during cogrinding and storage is mediated by amorphous phase., Pharm. Res. 23 (10) (2006) 2381–2392.
[14] S.L. Childs, L.J. Chyall, J.T. Dunlap, V.N. Smolenskaya, B.C. Stahly, P.G. Stahlyi, Crystal engineering approach to forming cocrystals of amine hydrochlorides with organic acids. Molecular complexes of fluoxetine hydrochloride with benzoic, succinic, and fumaric acids, J. Am. Chem. Soc. 126 (41) (2004) 13335–13342.
[15] S. Morissette, O. Almarsson, M. Peterson, J. Remenar, M. Read, A. Lemmo, S. Ellis, M. Cima, C. Gardner, High-throughput crystallization: polymorphs, salts, co-crystals and solvates of pharmaceutical solids, Adv. Drug Deliv. Rev. 56 (3) (2004) 275–300.
[16] D. McNamara, S. Childs, J. Giordano, A. Iarriccio, J. Cassidy, M. Shet, R. Mannion, E. O'Donnell, A. Park, Use of a glutaric acid cocrystal to improve oral bioavailability of a low solubility api, Pharm. Res. 23 (8) (2006) 1888–1897.
[17] S.L. Childs, P.G. Stahly, A. Park, The salt-cocrystal continuum: the influence of crystal structure on ionization state, Mol. Pharm. 4 (3) (2007) 323–338.
[18] S. Chow, M. Chen, L. Shi, C. Sun, Simultaneously improving the mechanical properties, dissolution performance, and hygroscopicity of ibuprofen and flurbiprofen by cocrystallization with nicotinamide, Pharm. Res. 29 (7) (2012) 1854–1865.
[19] N. Issa, P.G. Karamertzanis, G.W.A. Welch, S.L. Price, Can the formation of pharmaceutical cocrystals be computationally predicted? I. Comparison of lattice energies, Cryst. Growth Des. 9 (2009) 442–453.
[20] M. Etter, Hydrogen bonds as design elements in organic chemistry, J. Phys. Chem. 95 (12) (1991) 2586–2598.
[21] J.A. Zerkowski, J.C. MacDonald, C.T. Seto, D.A. Wierda, G.M. Whitesides, Design of organic structures in the solid state: molecular tapes based on the network of hydrogen bonds present in the cyanuric acid.cntdot.melamine complex, J. Am. Chem. Soc. 116 (6) (1994) 2382–2391.
[22] R. Pepinsky, Crystal engineering – new concept in crystallography, Phys. Rev. 100 (3) (1955), 971–971.
[23] H.-J. Werner, P.J. Knowles, G. Knizia, F.R. Manby, M. Schütz, Wires, Comput. Mol. Sci. 2 (2012) 242–253.
[24] A. Hesselmann, G. Jansen, M. Schütz, Density-functional theory-symmetry-adapted intermolecular perturbation theory with density fitting: a new efficient method to study intermolecular interaction energies, J. Chem. Phys. 122 (2005) 014103.
[25] G. Chałasiński, M.M. Szcześniak, Mol. Phys. 63 (1988) 205.
[26] G. Chałasinski, M.M. Szcześniak, Origins of structure and energetics of van der waals clusters from ab initio calculations, Chem. Rev. 94 (7) (1994) 1723–1765.
[27] R.W. Gora, W. Bartkowiak, S. Roszak, J. Leszczynski, A new theoretical insight into the nature of intermolecular interactions in the molecular crystal of urea, J. Chem. Phys. 117 (2002) 1031–1039.

[28] R.W. Gora, W. Bartkowiak, S. Roszak, J. Leszczynski, Intermolecular interactions in solution: elucidating the influence of the solvent, J. Chem. Phys. 120 (2004) 2802–2813.
[29] B. Jeziorski, M. van Hemert, Variation–perturbation treatment of the hydrogen bond between water molecules, Mol. Phys. 31 (1976) 713–729.
[30] M.W. Schmidt, K.K. Baldridge, J.A. Boatz, S.T. Elbert, M.S. Gordon, J.H. Jensen, S. Koseki, N. Matsunaga, K.A. Nguyen, S.J. Su, T.L. Windus, M. Dupuis, J.A. Montgomery, J. Comput. Chem. 14 (1993) 1347.
[31] R.W. Gora, EDS package, Revision 2.8.3, Wrocław, Poland (1998–2008).
[32] R.F.W. Bader, Atoms in Molecules, a Quantum Theory, Oxford University Press, Oxford, 1990.
[33] R.F.W. Bader, Chem. Rev. 91 (1991) 893.
[34] Designed by Friedrich Biegler-Konig, AIM2000 package, University of Applied Sciences, Bielefeld, Germany.
[35] R. Dovesi, V.R. Saunders, R. Roetti, R. Orlando, C.M. Zicovich-Wilson, F. Pascale, B. Civalleri, K. Doll, N.M. Harrison, I.J. Bush, P. D'Arco, M. Llunell, Crystal09, University of Torino, Torino 80.
[36] D. Feller, J. Comput. Chem. 17 (1996) 1571–1586.
[37] K.L. Schuchardt, B.T. Didier, T. Elsethagen, L. Sun, V. Gurumoorthi, J. Chase, J. Li, T.L. Windus, J. Chem. Inform. Model. 47 (2007) 1045–1052.
[38] S. Grimme, J. Comput. Chem. 27 (2006) 1787–1799.
[39] B. Civalleri, C.M. Zicovich-Wilson, L. Valenzano, P. Ugliengo, CrystEngComm 10 (4) (2008) 405–410.
[40] Y. Miwa, T. Mizuno, K. Tsuchida, Y. Tagaa, T. Iwata, Experimental charge density and electrostatic potential in nicotinamide, Acta Cryst. B55 (1999) 78–84.
[41] W.B. Wright, G.S.D. King, The crystal structure of nicotinamide, Acta Cryst. 7 (1954) 283–288.
[42] Ż. Czyżnikowska, R.W. Góra, R. Zaleśny, P. Lipkowski, K.N. Jarzembska, P.M. Dominiak, J. Leszczynski, Structural variability and the nature of intermolecular interactions in Watson–Crick B-DNA base pairs, J. Phys. Chem. B 114 (2010) 9629–9644.
[43] Z. Czyżnikowska, On the importance of electrostatics in stabilization of stacked guanine–adenine complexes appaearing in b-dna crystals, J. Mol. Struct. (THEOCHEM) (2009) 161–167.
[44] Z. Czyżnikowska, P. Lipkowski, R.W. Gora, R. Zaleśny, A.C. Cheng, On the nature of intermolecular interactions in nucleic acid base-amino acid side-chain complexes, J. Phys. Chem. B 113 (2009) 11511–11520.
[45] C.F. Matta, J. Hernandez-Trujillo, T.H. Tang, R.F.W. Bader, Hydrogen–hydrogen bonding: a stabilizing interaction in molecules and crystals, Chem. Eur. J. 9 (2003) 1940–1951.
[46] R.F.W. Bader, H. Essen, The characterization of atomic interactions, J. Chem. Phys. 80 (1984) 1943–1960.
[47] U. Koch, P.L.A. Popelier, Characterization of C—H—O hydrogen bonds on the basis of the charge density, J. Phys. Chem. 99 (1995) 9747–9754.